

Article

Thermodynamic Study of Phosphate Adsorption and Removal from Water Using Iron Oxyhydroxides

Kyriaki Kalaitzidou ^{1,*} , Anastasios Zouboulis ²  and Manassis Mitrakas ¹

¹ Department of Chemical Engineering, School of Engineering, Aristotle University of Thessaloniki, 54124 Thessaloniki, Greece; mmitraka@auth.gr

² Department of Chemistry, School of Sciences, Aristotle University of Thessaloniki, 54124 Thessaloniki, Greece; zoubouli@chem.auth.gr

* Correspondence: kalaitzidou@cheng.auth.gr

Abstract: Iron oxyhydroxides (FeOOHs) appear to be the optimal group of materials among inorganic adsorbents for the removal of phosphates from water, providing significant adsorption capacities. This research work presents a thermodynamic study of phosphate adsorption by examining five different FeOOHs sorbent nanomaterials. The obtained results indicated that the adsorption process in these cases was spontaneous. When the experiments were performed using distilled water, akaganeite (GEH), schwertmannite, and tetravalent manganese ferrioxalate (AquAsZero), displaying ΔH° values of 31.2, 34.7, and 7.3 kJ/mole, respectively, presented an endothermic adsorption process, whereas for goethite (Bayoxide) and lepidocrocite, with ΔH° values of -11.4 and -7.7 kJ/mole, respectively, the adsorption process proved to be exothermic. However, when an artificial (according to NSF) water matrix was used, GEH, schwertmannite, lepidocrocite, and AquAsZero presented ΔH° values of 13.2, 3.3, 7.7, and 3.3 kJ/mole, respectively, indicative of an endothermic process, while only for Bayoxide, with ΔH° of -17 kJ/mole, the adsorption remained exothermic. The adsorption enthalpy values generally decreased with the NSF water matrix, probably due to the competition for the same adsorption sites by other co-existing anions as well to the possible formation of soluble phosphate complexes with calcium; however, an overall positive effect on the uptake of phosphates was observed.

Keywords: phosphate adsorption; iron oxyhydroxides; thermodynamic parameters; adsorption isotherms; adsorption capacity



Citation: Kalaitzidou, K.; Zouboulis, A.; Mitrakas, M. Thermodynamic Study of Phosphate Adsorption and Removal from Water Using Iron Oxyhydroxides. *Water* **2022**, *14*, 1163. <https://doi.org/10.3390/w14071163>

Academic Editor: Gaurav Sharma

Received: 10 February 2022

Accepted: 4 April 2022

Published: 5 April 2022

Publisher's Note: MDPI stays neutral with regard to jurisdictional claims in published maps and institutional affiliations.



Copyright: © 2022 by the authors. Licensee MDPI, Basel, Switzerland. This article is an open access article distributed under the terms and conditions of the Creative Commons Attribution (CC BY) license (<https://creativecommons.org/licenses/by/4.0/>).

1. Introduction

The release of phosphorus, mainly through wastewaters in the aqueous environment, results in the acceleration/increase of eutrophication problems in aquatic ecosystems. Considering the lack of phosphorus in the soil (where it is applied as a fertilizer) and, on the other hand, its occasionally excessive content in water sources, which raises the eutrophication problem [1], it is essential to remove and recover phosphorus from alternative sources, considered nowadays as “wastes”, in a reusable form [2–5]. In this regard, the adsorption of anions, especially of phosphates, onto inorganic adsorbent materials is generally of great importance for regulating their concentrations in natural waters. In this case, the adsorption capacity is mainly regulated by the affinity of anions with the surface of the adsorbent media, the relative concentration of the anions, as well as the pH and the temperature of the process [6–8].

Granular solids formed by the spontaneous secondary aggregation of nanoparticles are widely applied in adsorption processes for the removal of pollutants [9]. Iron oxyhydroxides (FeOOHs) nanomaterials, with building units in the range of 2–10 nm [10–13], have attracted the attention of several researchers, due to their strong affinity to phosphates, along with other, mainly anionic aquatic hazardous species, such as arsenic oxy-anions.

This group of materials present quite large specific surface areas alongside with large heterogeneous surfaces, derived from (more or less) amorphous (mineralogical) phases, which can result in the maximum available ion-exchange/sorption sites. Such relation can be mainly attributed to the ligand exchange reaction that takes place onto the adsorbent's surface, i.e., in this case, between phosphate anions and the structural hydroxyl groups of respective surfaces [14–17]. The most commonly occurring FeOOHs solid phases are goethite (α -FeOOH), akageneite (β -FeOOH), lepidocrocite (γ -FeOOH), feroxyhyte (δ -FeOOH), and schwertmannite. Among the specific advantages of these materials there is their commercial availability at rather low costs, as well as their regeneration capacity, allowing their reuse [18–20].

Energy is either released or captured during the adsorption process. Depending on the system enthalpy, it can be determined whether adsorption would be of exothermic or endothermic nature, i.e., with positive or negative values, respectively [8]. In addition, more information regarding the adsorption mechanism can be obtained from the enthalpy values, as at the higher measured values (i.e., $\Delta H^\circ > 40$ kJ/mol), chemisorption takes place, with the formation of chemical bonds between the ions and the adsorbent material, whereas at intermediate values (i.e., 20 kJ/mol $< \Delta H^\circ < 40$ kJ/mol), weak chemisorption can take place and at the lower values (i.e., $\Delta H^\circ < 20$ kJ/mol), physisorption occurs with the formation of weak Van-der-Waal forces [20]. Moreover, the Gibbs free energy is also a measure of the work that can be produced by the adsorption system under constant temperature and pressure. Therefore, thermodynamic studies are usually performed in order to correlate the influence of temperature on the adsorption process, as well as the changes of the main thermodynamic parameters, including standard free energy (ΔG°), enthalpy (ΔH°), and entropy (ΔS°), of the examined adsorption system [20,21]. Thus, both thermodynamic and kinetic studies are essential for the design of appropriate adsorption processes in terms of energy and mass balance calculations and relevant construction considerations, respectively [8,20,21].

Relevant adsorption experiments, previously carried out by Saha et al. [22] for GEH (Granular Ferric Hydroxide), suggested an endothermic and spontaneous process occurring at pH 3, with a ΔH° value of 68.79 kJ/mole and a negative ΔG° value. Moreover, similar results regarding the adsorption of phosphate onto goethite were presented by Juang et al. [23] at pH 4.5, with a ΔH° value of 33.9 kJ/mole and ΔG° values of -9.8 , -12.1 , and -12.9 kJ/mole at temperatures of 288, 298, and 308 K, respectively. In accordance to these results, the study of Li et al. [24], regarding the adsorption of phosphate onto δ -FeOOH/Fe(II), also showed a ΔH° value of 15.75 kJ/mole occurring at pH 3 and at 298.15, 308.15, and 318.15 K. In contrast, Deliyanni et al. [25] calculated a ΔH° value of -12.2 kJ/mole for akageneite at pH 7, indicating an exothermic process.

As already mentioned, the adsorption onto the FeOOHs nanomaterials is a process that depends upon several parameters, as well as on the material's specific surface structure [14,22]. In a previous study, the pH effect of phosphate adsorption was investigated by using several FeOOHs materials in distilled, as well as in NSF (National Science Foundation) water matrix [17]. However, to the best of our knowledge, the main thermodynamic parameters, regarding the adsorption of phosphates by different FeOOHs samples, were not thoroughly investigated when applying conditions commonly encountered in natural waters and under comparable experimental conditions. The aim of this study was to evaluate the effect of temperature on the adsorption of phosphates by the most common FeOOHs sorbents at pH 7, as well as to calculate the respective thermodynamic parameters by using a distilled as well as an artificial (according to NSF, 789 N. Dixboro Road Ann Arbor, MI, USA) water matrix. Conditions similar to those of secondary wastewater treatment plant effluents were selected, aiming to produce results that can be potentially applied at a larger (pilot-) scale.

2. Materials and Methods

2.1. Examined Adsorbents

The main thermodynamic parameters were evaluated for the three commercially available FeOOHs sorbents, i.e., GEH (supplied by GEH Wasserchemie GmbH & Co. KG, Osnabrück, Germany) and Bayoxide (supplied by Lanxess, Cologne, Germany), consisting (nominally) of akaganeite and goethite, respectively, as well as for tetravalent manganese ferrioxhyte AquAsZero (supplied by Loufakis Chemicals S.A., Thessaloniki, Greece). In addition, we used two laboratory-synthesized iron oxyhydroxides, consisting of schwertmannite and lepidocrocite, prepared by using the oxidation–precipitation reaction of $\text{FeSO}_4 \cdot \text{H}_2\text{O}$ (supplied by Loufakis Chemicals S.A., Thessaloniki, Greece, >99.0% purity), under intensive oxidative conditions, and applying a two-step continuous flow process [8,13].

The iron and manganese content of the adsorbents was determined after sample dissolution in HCl by flame atomic absorption spectroscopy using a Perkin Elmer (Waltham, MA, USA), AAnalyst 800 instrument. The surface area and porosity of the adsorbent samples was estimated by nitrogen gas adsorption at liquid N_2 temperature (77 K) using a micropore surface area analyzer according to the Brunauer–Emmett–Teller (BET) model (Self-construction, Thessaloniki, Greece).

The Iso-Electric Point (IEP) was measured by using the water dispersion of each oxy-hydroxide solid and determined by the curve of zeta-potential values at $20 \pm 1^\circ \text{C}$. The sample preparation included the suspension of 50 mg of fine oxy-hydroxide powder from each material into 1 L of electrolyte solution (0.01 M NaNO_3 , supplied by Merck, Kenilworth, NJ, USA, >99.5% purity). Smaller quantities (100 mL) were equilibrated at different pH values (3–10) for 60 min by adding either HNO_3 (supplied by Chem-Lab, Zedelgem, Belgium, 65.0% purity) or NaOH (prepared using sodium hydroxide pellets, supplied by Chem-Lab, Zedelgem, Belgium, >99.0% purity), under continuous stirring. The electrophoretic velocity of at least 20 particles was then determined through a digital camera by using a Rank Brothers (Cambridge, United Kingdom), Micro-Electrophoresis Apparatus Mk II, and the respective z-potential value was calculated.

The surface charge density of the adsorbents and the Point of Zero Charge (PZC) were estimated using the potentiometric mass titration method [26].

The total sulfate content of FeOOHs was determined gravimetrically after precipitation as BaSO_4 [27]. We dissolved 200 mg of each material in 8 mL HCl (6N) supplied by Chem-Lab (Zedelgem, Belgium), 37% purity, by applying mild heating. Then, 150 mL of hot distilled water was added, followed by the drop-wise addition of 50 mL of a BaCl_2 solution (5 g/L) (supplied by Sigma-Aldrich, Burlington, MA, United States, >99% purity). The white precipitate of BaSO_4 was aged under heating for at least 2 h, filtered through a 0.45 μm pore-size fiberglass filter, dried, and weighed. The physically adsorbed sulfate was extracted with water, and both the physically and the chemically adsorbed sulfate were extracted with 5 mM NaOH and determined by an Alltech (Thessaloniki, Greece), 600 ion chromatography system, using a Transgenomic (Omaha, NE, USA), IC Sep AN1 column and a 1.7 mM NaHCO_3 /1.8 mM Na_2CO_3 solution as the eluent [28].

The main physicochemical parameters of the five adsorbents as examined comparatively in this manuscript are shown in Table 1. Moreover, K, Zn, Cu, Mg and Ca were found in minor quantities, <0.3 wt%, whereas NO_3^- , Cr, and Ni were not detected in the FeOOH materials.

2.2. Chemical Reagents

A phosphate stock solution (300 mg/L) was prepared by diluting 429.5 mg of anhydrous KH_2PO_4 (supplied by Panreac, Darmstadt, Germany, >98.0% purity) in 1 L of distilled water. The standard working solutions used for laboratory experiments was prepared by the appropriate dilution of the stock solution. The pH values of the phosphate solutions in distilled water were adjusted either by NaOH or by HCl addition, while 2 mM of N, N-Bis(2-hydroxyethyl)-2-amino-ethane-sulfonic acid reagent (denoted as BES and supplied by Alfa

Aesar, Karlsruhe, Germany, >99.0% purity) was used as the buffer system to facilitate the pH control. The artificial natural water, used in the experiments, was prepared according to the National Sanitation Foundation (NSF) standard and contained 252 mg of NaHCO₃ (supplied by Merck, Kenilworth, NJ, USA, >99.5% purity), 12.14 mg of NaNO₃ (supplied by Merck, Kenilworth, NJ, USA, >99.5% purity), 0.178 mg of NaH₂PO₄·H₂O (supplied by Sigma-Aldrich, Burlington, MA, USA, >98.0% purity), 2.21 mg of NaF (supplied by Merck, Kenilworth, NJ, USA, >99.0% purity), 70.6 mg of NaSiO₃·5H₂O (supplied by Loufakis Chemicals S.A., Thessaloniki, Greece, >99.0% purity), 147 mg of CaCl₂·2H₂O (supplied by Riedel-de Haen, Seelze, Germany, >99.0% purity), and 128.3 mg of MgSO₄·7H₂O (supplied by Panreac, Darmstadt, Germany, >98.0% purity), dissolved in 1 L of distilled water [29].

Table 1. Main physicochemical characteristics of five examined different iron oxyhydroxides materials.

Oxyhydroxide	Fe (wt.%)	Mn (wt.%)	Na (wt.%)	Physically Adsorbed	Chemically Adsorbed	Crystalline Structural	BET (m ² /g)	IEP ¹	ZPC ²	PSCD ³ (mmol [OH ⁻]/g)
				SO ₄ ²⁻ (wt.%)						
AquAsZero	38.3	11.8	3.5	5.9	5.3	1.5	205	7.2	3.2	2.6
Bayoxide	52.4	-	0.3	<0.2	<0.2	ND ⁴	135	7.4	7.8	0.8
GEH	54.2	-	0.5	<0.2	<0.2	ND	237	7.2	5.2	1.0
Lepidocrocite	50.6	-	3.5	5.7	2.3	ND	155	7.3	4.2	1.6
Schwertmannite	45.5	-	2.0	4.4	6.2	5.4	53	7.2	2.9	3.2

¹ Isoelectric Point, ² Point of Zero Charge, ³ Positive Surface Charge Density, ⁴ Not Detected.

2.3. Experimental Procedure

Batch adsorption experiments were carried out in order to record the respective isotherms and to evaluate the adsorbents' efficiency. We dispersed 15–70 mg of fine powdered (<63 μm) samples in 200 mL of phosphate solutions at pH 7, using 300 mL conical flasks. The flasks were placed in an orbital shaker (Widg Wiseshake SHO-2D supplied by Witeg Labortechnik GMBH, Wertheim, Germany) and stirred for 24 h at constant temperatures of 283, 293, and 308 K. After the set contact time to reach equilibrium (i.e., 24 h, according to preliminary experiments), the samples were filtered by using 0.45 μm membrane filters, and the residual (i.e., not adsorbed/removed) concentration of phosphates in the so-treated solutions was determined accordingly. All experiments were conducted in triplicates, and the average values are presented. The adsorbents were evaluated by calculating the respective adsorption capacity at the equilibrium (limit) concentration of 3 mg PO₄³⁻/L, which is abbreviated as Q₃, henceforth. The concentration limit of 3 mg PO₄³⁻/L was set by the Council Directive (1991) [30] as the regulation limit, regarding the content of phosphates in (treated) wastewaters before disposal and in environmentally sensitive aquatic areas.

The change of Gibbs free energy in the adsorption reaction was calculated by Equation (1):

$$\Delta G^{\circ} = -RT \ln K_{\text{ads}} \quad (1)$$

where R is the ideal gas constant (8.314 J/(mol K)), T is the absolute temperature in Kelvin, and K_{ads} is the equilibrium adsorption constant, which was calculated from the equilibrium constant of Langmuir K_L, when expressed as L/mol of phosphates [31]. ΔH[°] and ΔS[°] were calculated from the Van't-Hoff Equation (2):

$$\ln K_{\text{ads}} = -\frac{\Delta H^{\circ}}{RT} + \frac{\Delta S^{\circ}}{R} \quad (2)$$

By plotting ln(K_{ads}) versus 1/T, ΔH[°] and ΔS[°] were calculated from the slope and intercept of the linear equation, respectively [32].

Moreover, the kinetics of phosphates adsorption was evaluated by dispersing 200 mg of adsorbent in 1 L of 10 mg PO₄³⁻/L in NSF water matrix at pH 7 and at the three examined temperatures (283, 293, and 308 K). Sampling was performed frequently during the initial 2 h of treatment and, later, after more extended time intervals, when equilibrium was approaching.

The kinetic data are expressed by applying Equation (3) as a pseudo-second-order reaction [33]:

$$\frac{t}{Q_t} = \frac{1}{k_2 Q_e^2} + \frac{t}{Q_e} \quad (3)$$

where t is the examined contact time (min), Q_t is the adsorption capacity at this time (mg/g), Q_e is the adsorption capacity at equilibrium, and k_2 is the corresponding pseudo-second-order adsorption constant (g/mg·min). Furthermore, the kinetic data were also plotted according to the parabolic diffusion law [33]:

$$Q_t = k_1 \cdot t^{\frac{1}{2}} + a \quad (4)$$

where t is a constant in any experiment (mg/g).

2.4. Analytical Determination

The initial and residual concentrations of phosphates determined colorimetrically by applying the stannous chloride method (tin chloride (SnCl₂·2H₂O) was obtained using Panreac, >98.0% purity, mixed with glycerol that was supplied by Duchefa Biochemie, Haarlem, Netherlands, >98.0% purity, and ammonium molybdate ((NH₄)₆Mo₇O₂₄·4H₂O), supplied by Sigma-Aldrich, Burlington, MA, USA ≥99.0% purity, mixed with sulfuric acid (H₂SO₄) supplied by Chem-Lab, Zedelgem, Belgium, ≥95.0–97% purity) [34] at 690 nm and a UV-VIS Hitachi (Tokyo, Japan) U-5100 spectrophotometer.

3. Results and Discussion

3.1. Adsorption Isotherms

The adsorption isotherms reflect the equilibrium between the concentration of solutes (here, phosphates) in a solution and the corresponding value onto the surface of an adsorbent material at a given temperature. Most commonly, they are fitted according to either Freundlich or Langmuir models. Figure S1, Supplementary Materials, presents the experimental results of batch experiments regarding the studied FeOOHs sorbents at pH 7 and in the temperature range of 283–308 K, which was found to be better fitted according to the Freundlich model, in comparison with the Langmuir one. Moreover, adsorption was favored by increasing the temperature in the cases of the AquAsZero, GEH, and schwertmannite sorbents, both in distilled and in natural water (NSF) matrixes, an observation which confirms the endothermic character of this process. In contrast, the adsorption of phosphate by Bayoxide proved to be of exothermic nature. In the case of lepidocrocite, the adsorption of phosphate was decreased by the increase of temperature in distilled water, while it was favored (increased) in the NSF water matrix. The latter can probably be attributed to the adsorbed species of sulphate on the Stern layer of lepidocrocite that can be subsequently replaced by the adsorption of soluble calcium phosphate oxyanions, whose formation is favored when the pH is greater than 6, as seen in the respective speciation diagram (Figure 1) [13,35]. The distribution of phosphate species under the applied experimental conditions, for the NSF water matrix and for the initial concentration of phosphates of 10 mg/L at 293 K, showed that at pH > 6, the soluble calcium and magnesium phosphate oxyanions formed, which bound to a negatively charged anion; this subsequently reduced the overall negative charge in the aqueous solution, resulting in the positive effect of the NSF water matrix on the adsorption of phosphates, as observed for all the examined sorbent materials (see Table 2). In addition, it should be noted that the calculated Q_3 values from the Freundlich model were found to be similar to the Q_{\max} values, as they were calculated by the Langmuir model. In conclusion, AquAsZero showed the highest

Q_3 value (58 mg PO_4^{3-} /g) at 308 K with the NSF water matrix. As it has been already reported by Kalaitzidou et al., 2019, schwertmannite incorporates a higher percentage (5.4 wt.%) of SO_4^{2-} into a crystalline structure, when compared to AquAsZero (1.5 wt.%). Thus, schwertmannite has a slightly lower maximum adsorption capacity (Q_{\max}) than AquAsZero, probably due to its content of SO_4^{2-} anions in a crystalline structure, which possibly inhibit the binding of phosphate to schwertmannite, as reported for selenite [8]. In contrast, the adsorption capacity of schwertmannite appeared significantly greater than those of Bayoxide, GEH, and lepidocrocite, due to the high percentage of chemically adsorbed SO_4^{2-} anions (6.2 wt.%) that can be replaced by phosphate ions, because of their better affinity to the surface structure of the iron substrate.

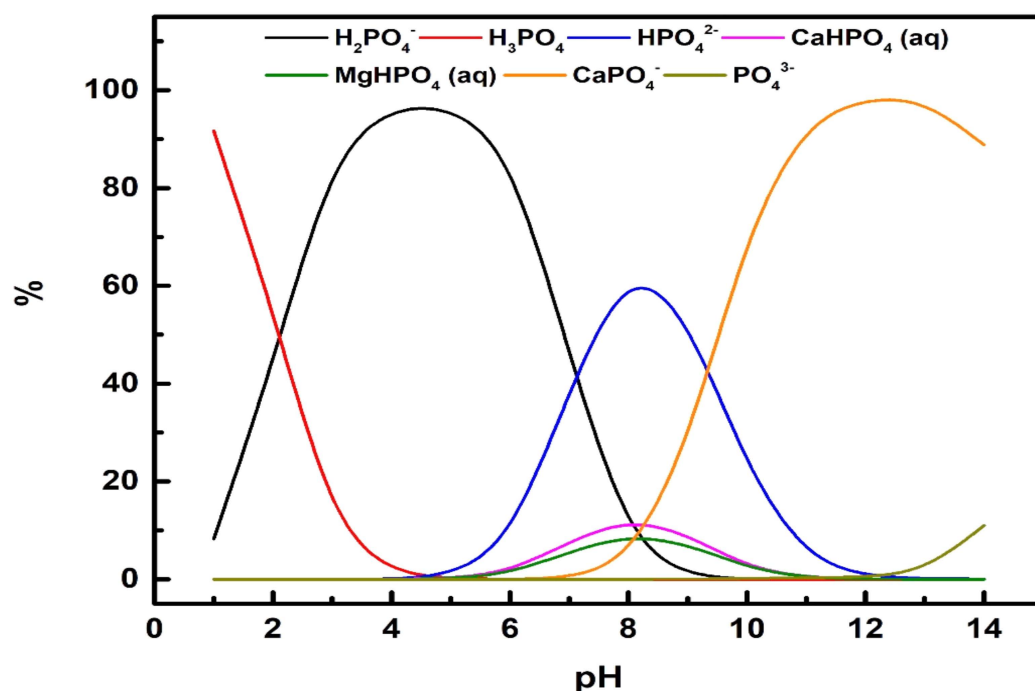


Figure 1. Speciation of the major PO_4^{3-} species using the NSF water matrix at an initial concentration of phosphates of 10 mg/L at 293 K; the respective diagrams were derived by using the Visual MINTEQ 3.0 software program (<http://vminteq.lwr.kth.se> (accessed on 15 December 2021)).

Table 2. Fitting parameters regarding the adsorption of phosphates at pH 7.

T (K)	LANGMUIR			FREUNDLICH			
	K_L (L/mg PO_4^{3-})	Q_{\max} (mg PO_4^{3-} /g)	R^2	Q_3 (mg PO_4^{3-} /g)	K_F (mg PO_4^{3-} /g)/(mg/L) ^{1/n}	1/n	R^2
<i>AquAsZero</i>							
<i>Distilled water</i>							
283	10.62	40.8	0.991	40.5	36.0	0.109	0.917
293	11.29	42.2	0.959	42.3	37.8	0.103	0.946
308	13.61	44.6	0.983	44.2	40.4	0.083	0.955
<i>NSF water</i>							
283	2.89	50.1	0.910	46.3	35.0	0.253	0.99
293	3.15	58.6	0.957	54.5	41.8	0.242	0.989
308	3.17	63.6	0.956	58.0	45.2	0.226	0.973

Table 2. Cont.

T (K)	LANGMUIR			FREUNDLICH			
	K_L (L/mg PO_4^{3-})	Q_{max} (mg PO_4^{3-} /g)	R^2	Q_3 (mg PO_4^{3-} /g)	K_F (mg PO_4^{3-} /g)/(mg/L) ^{1/n}	1/n	R^2
<i>Bayoxide</i>							
<i>Distilled water</i>							
283	16.37	20.2	0.867	23.0	18.5	0.200	0.994
293	15.64	18.7	0.744	19.4	17.2	0.109	0.98
308	11.17	17.9	0.952	18.1	15.9	0.120	0.978
<i>NSF water</i>							
283	8.38	23.7	0.967	24.7	20.4	0.173	0.979
293	5.58	24.4	0.931	24.2	19.8	0.185	0.996
308	4.58	24.4	0.960	23.6	19.2	0.187	0.969
<i>GFH</i>							
<i>Distilled water</i>							
283	11.44	30.5	0.963	33.1	27.1	0.183	0.977
293	15.42	28.4	0.933	30.1	25.6	0.149	0.994
308	12.94	27.7	0.954	29.3	24.6	0.159	0.975
<i>NSF water</i>							
283	11.65	30.0	0.965	32.5	26.7	0.180	0.975
293	12.86	31.0	0.862	33.4	27.9	0.163	0.997
308	32.96	31.6	0.808	34.7	29.8	0.139	0.993
<i>Lepidocrocite</i>							
<i>Distilled water</i>							
283	17.5	42.3	0.827	43.5	38.1	0.121	0.952
293	13.3	41.7	0.854	40.8	36.6	0.101	0.985
308	13.2	39.3	0.913	40.1	35.2	0.117	0.989
<i>NSF water</i>							
283	3.16	47.4	0.998	43.5	34.9	0.200	0.931
293	3.90	49.4	0.936	45.7	37.1	0.190	0.974
308	4.16	54.1	0.967	51.2	40.6	0.213	0.982
<i>Schwertmannite</i>							
<i>Distilled water</i>							
283	18.79	44.2	0.883	47.8	41.5	0.129	0.995
293	40.15	45.7	0.869	51.9	45.7	0.116	0.977
308	63.85	46.6	0.686	51.6	46.5	0.096	0.983
<i>NSF water</i>							
283	2.61	53.0	0.909	50.0	36.3	0.291	0.975
293	2.63	57.2	0.952	52.1	39.0	0.263	0.999
308	2.92	59.2	0.974	54.8	41.3	0.259	0.991

3.2. Thermodynamic Parameters

The effect of temperature on the efficiency and the strength of phosphate adsorption onto FeOOHs sorbent materials may be explained by considering the major thermodynamic parameters, such as Gibbs free energy (ΔG°), enthalpy (ΔH°), and entropy (ΔS°) of this process. ΔH° and ΔS° were calculated and are presented in Table 3.

Table 3. Summary of the major thermodynamic parameters for all the five examined adsorbents.

Oxyhydroxides	ΔH° (kJ/mol)	ΔS° (J/mol·K)	$-\Delta G^\circ$ (kJ/mol)		
			283 K	293 K	308 K
Distilled water					
AquAsZero	7.3	140.6	33	34	36
Bayoxide	−11.4	78.5	34	35	36
GEH	31.2	224.8	33	34	38
Lepidocrocite	−7.7	91.3	33	34	35
Schwertmannite	34.7	243.1	34	37	40
NSF water					
AquAsZero	2.6	113.5	30	31	32
Bayoxide	−17.0	52.0	32	32	33
GEH	13.2	150.1	29	30	33
Lepidocrocite	7.7	132.2	30	31	33
Schwertmannite	3.3	114.8	29	30	32

Moreover, by plotting $\ln(K_{ads})$ versus $1/T$, the ΔH° and ΔS° values were calculated from the slope and the intercept of the linear equation, respectively (Figure 2).

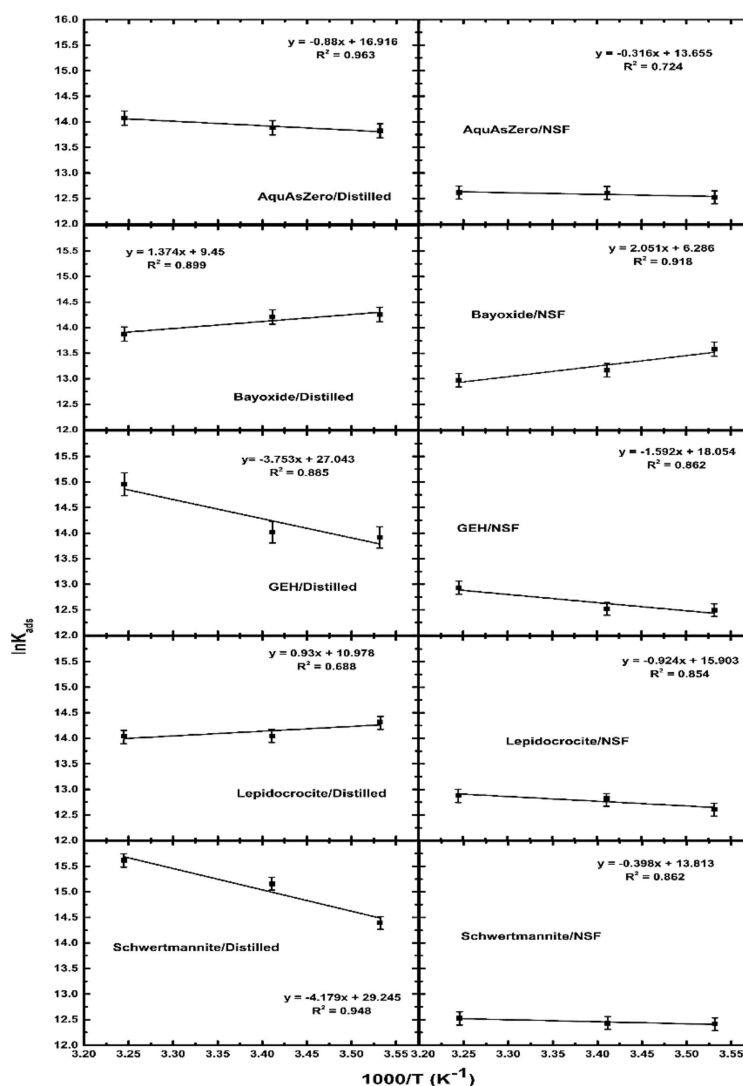


Figure 2. Van't Hoff plots of phosphate adsorption data in the examined experimental conditions.

The observed negative values of ΔG° (Table 3) indicated the spontaneous nature of phosphate adsorption, whereas the positive values of ΔS° indicated an increased randomness at the solid/solution interface [36]. The calculated ΔH° values for phosphate uptake in a low equilibrium concentration range (0.3–4 mg phosphates/L) in distilled water indicated an endothermic weak chemisorption reaction for GFH and schwertmannite and an endothermic physisorption reaction for AquAsZero, while phosphate uptake from Bayoxide and lepidocrocite proceeded mainly through an exothermic physisorption reaction (Table 3).

The results of the thermodynamic study for the GEH material are in accordance with the results of Saha et al. [22], who showed that an increase of pH from 3 to 4 reduced the ΔH° and ΔG° values, although it has to be noticed that the results of the current study were obtained at pH 7, at which the ΔH° and ΔG° values are expected to be lower. However, Deliyianni et al. [25] also examined akaganeite at the temperatures of 298, 318, and 338 K at pH 7 and at initial phosphate concentrations in the range of 10–300 mg/L, reporting different results (i.e., ΔH° value -12.2 kJ/mole) from those obtained in this study (i.e., a ΔH° value of 31.2 kJ/mole), which can be attributed to the different applied experimental conditions. Finally, as already mentioned, Juang et al. [23] reported a ΔH° value of 33.9 kJ/mol for goethite at pH 4.5, whereas for Bayoxide at pH 7, $\Delta H^\circ = -11.4$, indicating that at lower pH values, chemisorption occurs mainly due to a higher positive surface charge, but the increase of pH close to the IEP value results in physisorption, with the formation of weak Van-der-Waal bonds.

In contrast, the uptake of phosphate by the examined FeOOHs materials, when using the NSF water matrix, proceeds mainly through the physisorption mechanism; it is endothermic for AquAsZero, GEH, lepidocrocite, and schwertmannite and exothermic for Bayoxide. The physisorption of phosphate in the NSF water matrix should be probably attributed to the formation of calcium phosphate soluble complexes (Figure 1), which present lower affinity for the structural iron octahedral structure of FeOOHs. However, the weaker forces of phosphates' physisorption can favor the regeneration (and potential reuse) of FeOOHs sorbents, e.g., by using a 0.2–1 N NaOH solution as the reagent for the elution of phosphates, since the respective binding energy is quite small, and strong chemical bonds are not present, which in turn can lead to the eventual recovery of phosphates as the respective calcium salts after appropriate precipitation [8,17]. The easy and repeated regeneration of FeOOHs materials after the adsorption of phosphates was previously reported [17], verifying that the presence of physisorption weaker forces can favor the efficiency of this process.

The equilibrium constant K_w of water depends on the temperature and varies according to an endothermic reaction, i.e., it increases, when increasing the temperature.

$$K_w = [H^+][OH^-]$$

Thus, regarding the examined materials (FeOOHs):

- ✓ Bayoxide, consisting of goethite (α -FeOOH), was affected by the relatively low temperature rise, as the water equilibrium ($H_2O \rightarrow [H^+] + [OH^-]$) and the surface hydroxyl groups ($FeO-OH^+$) led to the decrease of the positive surface charge for both distilled and NSF water matrixes. Therefore, the increase of temperature did not favor the adsorption of phosphates in this case, indicating an exothermic adsorption.
- ✓ For AquAsZero and schwertmannite, due to the presence of chemically adsorbed (5.3 wt.%, and 6.2 wt.%, respectively) and structurally crystalline (1.5 wt.%, 5.4 wt.%, respectively) sulfate ions, the increase of temperature favored ions solubility from the crystalline structure, resulting in the increase of the positive surface charge when both distilled or NSF water matrixes were examined. Therefore, in these cases, the increase of temperature favored the increase of phosphates adsorption, resulting in endothermic adsorption. Similarly, GEH, consisting of akaganeite (β -FeOOH), contains channels in which Cl^- ions are stabilized by hydrogen bonding [18]. Thus,

- an increase of temperature in this case increased the solubility of the chloride ions, favoring the adsorption of phosphates and resulting in endothermic adsorption.
- ✓ Regarding Lepidocrocite (γ -FeOOH), it does not contain any structural sulfate ions but has a low content of chemically adsorbed sulfate ions (2.3 wt.%). Similarly to the Bay-oxide material, when the applied matrix was distilled water, the desorption of sulfate ions was not favored; hence, an increase of temperature shifted the equilibrium of the aqueous phase and affected the surface hydroxy groups (FeO-OH^+), thereby resulting in the reduction of the positive surface charge. Thus, the adsorption of phosphates was reduced, resulting in exothermic adsorption. In contrast, the presence of calcium in the NSF water, due to its relevant chemical affinity (i.e., $\text{Ca(II)} + \text{SO}_4^{2-} \leftrightarrow \text{CaSO}_4$), can favor the desorption of chemically adsorbed sulfate ions and, hence, increases the positive surface charge by favoring the adsorption of phosphates, resulting in endothermic adsorption.

3.3. Kinetic Study at the Different Applied Temperatures

The evaluation of the effect of contact time on the uptake rate at the three different examined temperatures (283, 293, and 308 K) was examined specifically for schwertmannite, due to its higher positive surface charge density. The adsorption data in relation to contact time for this material showed that at least 1 h contact time was required to reach 90% removal of phosphates at all the examined temperatures, with the highest temperature (308 K) showing a slightly better uptake rate (Figure 3). The respective equations derived from the fitting of the kinetics results to a pseudo-second-order reaction at the different temperatures examined are presented in Table 4.

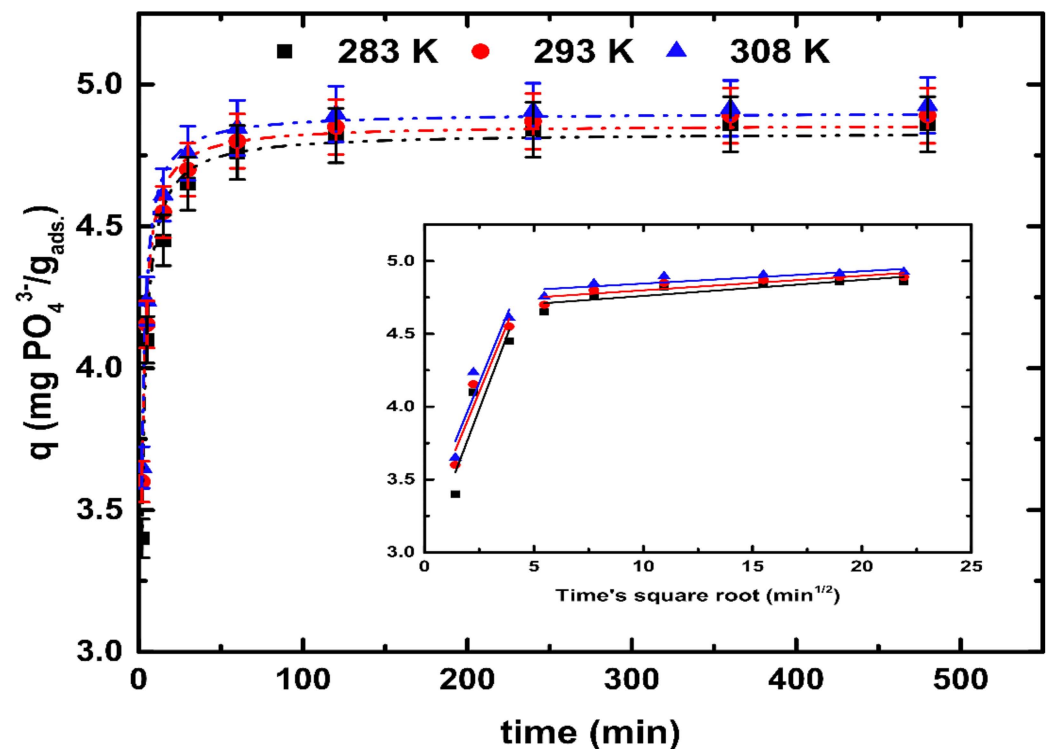


Figure 3. Kinetics data for the adsorption of phosphates onto schwertmannite in NSF water at pH 7 (C_0 : $10 \text{ mg PO}_4^{3-}/\text{L}$, schwertmannite dose 200 mg/L). In the insert diagram of this figure, the results from the application of the parabolic diffusion law are presented.

Table 4. Equations and fitting parameters derived from the kinetics adsorption data of schwertmannite oxyhydroxides.

Temperature	Pseudo-Second-Order Kinetic				Parabolic Diffusion Law	
	Equation	R ²	Q _e (mg/g)	k ₂ (g/(mg·min))	Equation	R ²
283 K	$Q = \frac{4.83t}{1+5.529t}$	0.988	3.9	0.3171	$Q = 0.397t^{1/2}+2.988$	0.863
293 K	$Q = \frac{4.858t}{1+6.508t}$	0.984	4.5	0.2503	$Q = 0.366t^{1/2}+3.184$	0.921
308 K	$Q = \frac{4.901t}{1+6.82t}$	0.991	5.1	0.1912	$Q = 0.368t^{1/2}+3.244$	0.904

The fitting parameters Q_e and k_2 were estimated to be 3.9, 4.5, and 5.1 mg/g and 0.3171, 0.2503, and 0.1912 g/(mg·min) at the three examined temperatures of 283, 293, and 308 K, respectively (Table 4). As the adsorption capacity at equilibrium (Q_e) increased with the increase of temperature, the respective pseudo-second-order adsorption constant (k_2) decreased. Since the schwertmannite sample was mainly composed of porous particles that were vigorously agitated during the adsorption period, it is logical to assume that the adsorption rate was not limited by the mass transfer rate from the bulk liquid to the particle external surface. However, the phosphate ions are able to diffuse into the pore channels of mesoporous materials, such as schwertmannite, which present a mean pore diameter of 47 Å [13].

To verify this assumption, the amount of adsorbed phosphates (Q_t at time t) was also plotted (see Figure 3, insert) according to the parabolic diffusion law.

The effect of intra-particle diffusion on the adsorption process corresponds to the linear portion (Figure 3, insert) of the curve, and the plateau to the respective equilibrium stage. The fact that the linear part of the curve does not pass through the origin indicates that the intra-particle diffusion was not the only rate-controlling parameter, regarding the adsorption of phosphates onto schwertmannite. The k_i values shown in Table 4 (0.397, 0.366, and 0.368 $\mu\text{g mg}^{-1}\text{min}^{-1/2}$) for the kinetic study at the temperatures of 283, 293, and 308 K, respectively, were calculated from the slope of the linear portion of the respective curves (Figure 3, insert). It is obvious from the similar k_i values that the different applied temperatures in the range of 283–308 K led to quite similar results with respect to the adsorption kinetics of phosphates onto the FeOOH schwertmannite material. As the adsorption process of phosphates onto schwertmannite is actually a two-step process, fast adsorption can be mainly attributed to boundary layer diffusion or macro-pore diffusion, and slow adsorption to the intra-particle diffusion or micro-pore diffusion [37].

4. Conclusions

The thermodynamic study of phosphate adsorption onto five different iron oxyhydroxides (FeOOHs) nanomaterials showed that the Freundlich model and the pseudo-second-order kinetic model can provide the best description of the adsorption isotherm and kinetics, respectively. The ΔH° values are mainly affected by the presence of chemically adsorbed sulfates or chloride ions in the examined iron-based materials, which appear to be actively involved in the anion exchange process with phosphates and to be differently influenced by temperature, allowing either an endothermic or an exothermic adsorption of phosphates, due to the overall effect on the positive surface charge. Moreover, the negative values of ΔG° illustrate the spontaneous nature of phosphates adsorption, whereas the positive values of ΔS° suggests the increased randomness at the solid/solution interface.

This work provides evidence of the significant effect that the presence of natural water has on the adsorption of phosphates, regarding the examination of different (but commonly examined and, some of them, commercially available) iron-based (FeOOHs) nanomaterials at the equilibrium pH 7. More specifically, the adsorption capacities (expressed as Q_3) at 293 K and when artificial NSF was used ranged between the lowest value of 24.2 mg/kg for Bayoxide and the optimum (highest) one of 54.5 mg/kg for AquAsZero. The fact that the optimal positive surface charge density that was reported for schwertmannite resulted in the best adsorption of phosphate, when using distilled water, was due to the dissolution of

sulfates in crystalline structure, while the presence of NSF water seemed to (slightly) inhibit the dissolution of structurally crystalline sulfates, thus lowering the positive surface charge density, which in turn negatively influenced the adsorption of phosphates, resulting in a slightly lower adsorption capacity of the rest of the examined materials, when compared to AquAsZero. The presence of several ions in natural waters can enhance a weaker phosphate uptake capacity through the physisorption mechanism, which is most probably due to the formation of calcium phosphate soluble complexes. However, the weakly applied forces of physisorption can also favor the regeneration of used FeOOHs nanomaterials by applying an alkaline environment, as well as lead to the recovery and potential reuse of the removed phosphates, explaining the results reported in a previous study.

Finally, the results of the kinetics study regarding the adsorption of phosphates onto schwertmannite showed that the uptake rate was slightly favored by the increase of temperature; in addition, it was not limited by the relevant mass transfer rate, but rather by the intra-particle diffusion step. This study provides important data regarding the potential of FeOOHs nanomaterials as cost-effective adsorbents for the removal and potential recovery of phosphates at a pilot or even at a large scale from contaminated waters or from wastewater effluents after secondary treatment.

Supplementary Materials: The following supporting information can be downloaded at: <https://www.mdpi.com/article/10.3390/w14071163/s1>, Figure S1. Phosphate adsorption isotherms at pH value 7, fitted by the Freundlich (—) or Langmuir main adsorption models (---).

Author Contributions: Conceptualization, A.Z. and M.M.; methodology, M.M.; validation, K.K.; formal analysis, K.K.; investigation, K.K.; resources, A.Z.; data curation, K.K.; writing—original draft preparation, K.K.; writing—review and editing, A.Z. and M.M.; visualization, A.Z.; supervision, M.M.; project administration, M.M.; funding acquisition, A.Z. All authors have read and agreed to the published version of the manuscript.

Funding: This research was co-financed by the European Union and the Greek State Program PAVET, Project (PhoReSE) Recovery of Phosphorus from the Secondary Effluent of Municipal Wastewater Treatment. Funding number 1525-BET-2013.

Institutional Review Board Statement: Not applicable.

Informed Consent Statement: Not applicable.

Data Availability Statement: The authors confirm that the data supporting the findings of this study are available within the article. Raw data that support the findings of this study are available from the corresponding authors, upon reasonable request.

Acknowledgments: This research project was approved by EYATH's S.A.—Department of Plants' Operation, Maintenance & Environmental Monitoring, which is gratefully appreciated.

Conflicts of Interest: The authors declare no conflict of interest.

References

1. Lee, J.-I.; Oh, J.-S.; Yoo, S.-C.; Jho, E.H.; Lee, C.-G.; Park, S.-J. Removal of phosphorus from water using calcium-rich organic waste and its potential as a fertilizer for rice growth. *J. Environ. Chem. Eng.* **2022**, *10*, 107367. [[CrossRef](#)]
2. Keyikoglu, R.; Khatae, A.; Yoon, Y. Layered double hydroxides for removing and recovering phosphate: Recent advances and future directions. *Adv. Colloid Interface Sci.* **2022**, *300*, 102598. [[CrossRef](#)]
3. Kunhikrishnan, A.; Rahman, M.A.; Lamb, D.; Bolan, N.S.; Saggar, S.; Surapaneni, A.; Chen, C. Rare earth elements (REE) for the removal and recovery of phosphorus: A review. *Chemosphere* **2022**, *286*, 131661. [[CrossRef](#)]
4. Lalley, J.; Han, C.; Mohan, R.G.; Dionysiou, D.D.; Speth, T.; Garland, J.; Nadagouda, N.M. Phosphate adsorption using modified iron oxide-based sorbents in lake water: Kinetics, equilibrium, and column tests. *Chem. Eng. J.* **2016**, *284*, 1386–1396. [[CrossRef](#)]
5. Raptopoulou, C.; Kalaitzidou, K.; Tolkou, A.; Palasantza, P.-A.; Mitrakas, M.; Zouboulis, A. Phosphate Removal from Effluent of Secondary Wastewater Treatment: Characterization of Recovered Precipitates and Potential Re-use as Fertilizer. *Waste Biomass Valorization* **2016**, *7*, 850–860. [[CrossRef](#)]
6. Kwon, K.; Kubicki, J. Molecular Orbital Theory Study on Surface Complex Structures of Phosphates to Iron Hydroxides: Calculation of Vibrational Frequencies and Adsorption Energies. *Langmuir* **2004**, *20*, 9249–9254. [[CrossRef](#)] [[PubMed](#)]

7. Sun, J.; Gao, A.; Wang, X.; Xu, X.; Song, J. Removal of Phosphorus from Wastewater by Different Morphological Alumina. *Molecules* **2020**, *25*, 3092. [[CrossRef](#)]
8. Kalaitzidou, K.; Nikolettopoulos, A.-A.; Tsiftsakos, N.; Pinakidou, F.; Mitrakas, M. Adsorption of Se(IV) and Se(VI) species by iron oxyhydroxides: Effect of positive surface charge density. *Sci. Total Environ.* **2019**, *687*, 1197–1206. [[CrossRef](#)]
9. Zhang, W. Nanoparticle aggregation: Principles and modeling. *Adv. Exp. Med. Biol.* **2014**, *811*, 19–43. [[CrossRef](#)]
10. Abid, A.D.; Kanematsu, M.; Young, T.M.; Kennedy, I.M. Arsenic removal from water using flame-synthesized iron oxide nanoparticles with variable oxidation states. *Aerosol. Sci. Technol.* **2013**, *47*, 169–176. [[CrossRef](#)]
11. Deliyanni, E.A.; Bakoyannakis, D.N.; Zouboulis, A.I.; Matis, K.A.; Nalbandian, L. Akaganéite-type β -FeO(OH) nanocrystals: Preparation and characterization. *Microporous Mesoporous Mater.* **2001**, *42*, 49–57. [[CrossRef](#)]
12. Tresintsi, S.; Simeonidis, K.; Estradé, S.; Martinez-Boubeta, C.; Vourlias, G.; Pinakidou, F.; Katsikini, M.; Paloura, E.C.; Stavropoulos, G.; Mitrakas, M. Tetravalent manganese ferrihydroxide: A novel nanoadsorbent equally selective for As(III) and As(V) removal from drinking water. *Environ. Sci. Technol.* **2013**, *47*, 9699–9705. [[CrossRef](#)]
13. Tresintsi, S.; Simeonidis, K.; Vourlias, G.; Stavropoulos, G.; Mitrakas, M. Kilogram-scale synthesis of iron oxyhydroxides with improved arsenic removal capacity: Study of Fe(II) oxidation-precipitation parameters. *Water Res.* **2012**, *46*, 5255–5267. [[CrossRef](#)]
14. Zhong, B.; Stanforth, R.; Wu, S.; Chen, J. Proton interaction in phosphate adsorption onto goethite. *J. Colloid Interface Sci.* **2007**, *308*, 40–48. [[CrossRef](#)]
15. Zhang, X.; Yao, H.; Lei, X.; Lian, Q.; Roy, A.; Doucet, D.; Yan, H.; Zappi, M.E.; Gang, D.D. A comparative study for phosphate adsorption on amorphous FeOOH and goethite (α -FeOOH): An investigation of relationship between the surface chemistry and structure. *Environ. Res.* **2021**, *199*, 111223. [[CrossRef](#)]
16. Ajmal, Z.; Muhmood, A.; Usman, M.; Kizito, S.; Lu, J.; Dong, R.; Wu, S. Phosphate removal from aqueous solution using iron oxides: Adsorption, desorption and regeneration characteristics. *J. Colloid Interface Sci.* **2018**, *528*, 145–155. [[CrossRef](#)]
17. Kalaitzidou, K.; Mitrakas, M.; Raptopoulou, C.; Tolkou, A.; Palasantza, P.-A.; Zouboulis, A. Pilot-Scale Phosphate Recovery from Secondary Wastewater Effluents. *Environ. Process.* **2016**, *3*, 5–22. [[CrossRef](#)]
18. Song, X.; Boily, J.F. Competitive ligand exchange on akaganéite surfaces enriches bulk chloride loadings. *J. Colloid Interface Sci.* **2012**, *376*, 331–333. [[CrossRef](#)]
19. Kalaitzidou, K.; Zouboulis, A.; Mitrakas, M. Cost evaluation for Se(IV) removal, by applying common drinking water treatment processes: Coagulation/precipitation or adsorption. *J. Environ. Chem. Eng.* **2020**, *8*, 104209. [[CrossRef](#)]
20. Saha, P.; Chowdhury, S. Insight Into Adsorption Thermodynamics. *Thermodynamics* **2011**, *16*, 349–364.
21. Kokkinos, E.; Soukakos, K.; Kostoglou, M.; Mitrakas, M. Cadmium, mercury, and nickel adsorption by tetravalent manganese ferrihydroxide: Selectivity, kinetic modeling, and thermodynamic study. *Environ. Sci. Pollut. Res.* **2018**, *25*, 12263–12273. [[CrossRef](#)] [[PubMed](#)]
22. Saha, B.; Griffin, L.; Blunden, H. Adsorptive separation of phosphate oxyanion from aqueous solution using an inorganic adsorbent. *Environ. Geochem. Health* **2010**, *32*, 341–347. [[CrossRef](#)] [[PubMed](#)]
23. Juang, R.S.; Chung, J.Y. Equilibrium sorption of heavy metals and phosphate from single- and binary-sorbate solutions on goethite. *J. Colloid Interface Sci.* **2004**, *275*, 53–60. [[CrossRef](#)] [[PubMed](#)]
24. Li, Y.; Fu, F.; Cai, W.; Tang, B. Synergistic effect of mesoporous ferrihydroxide nanoparticles and Fe(II) on phosphate immobilization: Adsorption and chemical precipitation. *Powder Technol.* **2019**, *345*, 786–795. [[CrossRef](#)]
25. Deliyanni, E.A.; Peleka, E.N.; Lazaridis, N.K. Comparative study of phosphates removal from aqueous solutions by nanocrystalline akaganéite and hybrid surfactant-akaganéite. *Sep. Purif. Technol.* **2007**, *52*, 478–486. [[CrossRef](#)]
26. Kosmulski, M. *Surface Charging and Points of Zero Charge*; CRC Press: Boca Raton, FL, USA, 2009; ISBN 9781420051896.
27. Vogel, A.I.; Mendham, J.; Denney, R.C.; Barnes, J.D.; Thomas, M. *Vogel's Quantitative Chemical Analysis*, 6th ed.; Prentice Hall: Essex, UK, 2000.
28. Tresintsi, S.; Simeonidis, K.; Pliatsikas, N.; Vourlias, G.; Patsalas, P.; Mitrakas, M. The role of so 4 2—Surface distribution in arsenic removal by iron oxy-hydroxides. *J. Solid State Chem.* **2014**, *213*, 145–151. [[CrossRef](#)]
29. Amy, G.; Chen, H.W.; Drizo, A.; von Gunten, U.; Brandhuber, P.; Hund, R.; Chowdhury, Z.; Kommineni, S.; Sinha, S.; Jekel, M.; et al. *Adsorbent Treatment Technologies for Arsenic Removal*; AWWA Research Foundation and American Water Works Association: Washington, DC, USA, 2005.
30. European Economic Community (EEC). Council Council Directive of 21 May 1991 concerning urban waste water treatment (91/271/EEC). *Off. J. Eur. Commu.* **1991**, *34*, 40, L 135.
31. Ramesh, A.; Lee, D.J.; Wong, J.W.C. Thermodynamic parameters for adsorption equilibrium of heavy metals and dyes from wastewater with low-cost adsorbents. *J. Colloid Interface Sci.* **2005**, *291*, 588–592. [[CrossRef](#)]
32. Chang, R. Physical chemistry for the chemical and biological sciences. *J. Chem. Educ.* **2001**, *78*, 594.
33. Unuabonah, E.I.; Omorogie, M.O.; Oladoja, N.A. Modeling in adsorption: Fundamentals and applications. In *Composite Nanoadsorbents*; Elsevier: Amsterdam, The Netherlands, 2019. [[CrossRef](#)]
34. APHA. *Standard Methods for the Examination of Water and Wastewater*, 22nd ed.; American Public Health Association: Washington, DC, USA, 2012. [[CrossRef](#)]
35. You, X.; Guaya, D.; Farran, A.; Valderrama, C.; Cortina, J.L. Phosphate removal from aqueous solution using a hybrid impregnated polymeric sorbent containing hydrated ferric oxide (HFO). *J. Chem. Technol. Biotechnol.* **2016**, *91*, 693–704. [[CrossRef](#)]

36. Das, J.; Patra, B.S.; Baliarsingh, N.; Parida, K.M. Adsorption of phosphate by layered double hydroxides in aqueous solutions. *Appl. Clay Sci.* **2006**, *32*, 252–260. [[CrossRef](#)]
37. Pan, M.; Lin, X.; Xie, J.; Huang, X. Kinetic, equilibrium and thermodynamic studies for phosphate adsorption on aluminum hydroxide modified palygorskite nano-composites. *RSC Adv.* **2017**, *7*, 4492–4500. [[CrossRef](#)]